



## NRC Publications Archive Archives des publications du CNRC

### **CO<sub>2</sub> adsorption on PIMs studied with <sup>13</sup>C NMR spectroscopy**

Moore, Jeremy K.; Marti, Robert M.; Guiver, Michael D.; Du, Naiying;  
Conradi, Mark S.; Hayes, Sophia E.

This publication could be one of several versions: author's original, accepted manuscript or the publisher's version. /  
La version de cette publication peut être l'une des suivantes : la version prépublication de l'auteur, la version  
acceptée du manuscrit ou la version de l'éditeur.

For the publisher's version, please access the DOI link below. / Pour consulter la version de l'éditeur, utilisez le lien  
DOI ci-dessous.

#### **Publisher's version / Version de l'éditeur:**

<https://doi.org/10.1021/acs.jpcc.7b12312>

*The Journal of Physical Chemistry C*, 122, 8, pp. 4403-4408, 2018-02-07

#### **NRC Publications Record / Notice d'Archives des publications de CNRC:**

<https://nrc-publications.canada.ca/eng/view/object/?id=7e26dbfb-60a8-494f-b44f-e582d25251f8>

<https://publications-cnrc.canada.ca/fra/voir/objet/?id=7e26dbfb-60a8-494f-b44f-e582d25251f8>

Access and use of this website and the material on it are subject to the Terms and Conditions set forth at

<https://nrc-publications.canada.ca/eng/copyright>

READ THESE TERMS AND CONDITIONS CAREFULLY BEFORE USING THIS WEBSITE.

L'accès à ce site Web et l'utilisation de son contenu sont assujettis aux conditions présentées dans le site

<https://publications-cnrc.canada.ca/fra/droits>

LISEZ CES CONDITIONS ATTENTIVEMENT AVANT D'UTILISER CE SITE WEB.

**Questions?** Contact the NRC Publications Archive team at

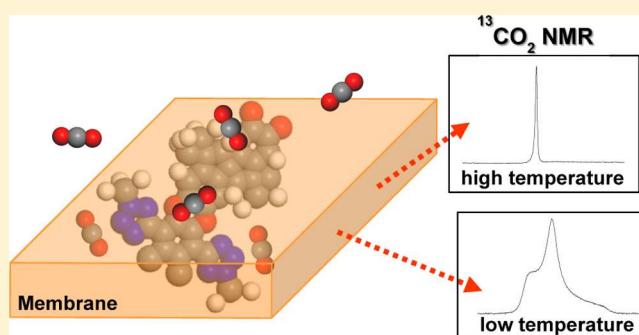
PublicationsArchive-ArchivesPublications@nrc-cnrc.gc.ca. If you wish to email the authors directly, please see the  
first page of the publication for their contact information.

**Vous avez des questions?** Nous pouvons vous aider. Pour communiquer directement avec un auteur, consultez la  
première page de la revue dans laquelle son article a été publié afin de trouver ses coordonnées. Si vous n'arrivez  
pas à les repérer, communiquez avec nous à PublicationsArchive-ArchivesPublications@nrc-cnrc.gc.ca.



CO<sub>2</sub> Adsorption on PIMs Studied with <sup>13</sup>C NMR SpectroscopyJeremy K. Moore,<sup>†</sup> Robert M. Marti,<sup>†</sup> Michael D. Guiver,<sup>§,||</sup> Naiying Du,<sup>⊥</sup> Mark S. Conradi,<sup>‡,#</sup> and Sophia E. Hayes<sup>\*,†,||</sup><sup>†</sup>Department of Chemistry and <sup>‡</sup>Department of Physics, Washington University, One Brookings Drive, Saint Louis, Missouri 63130, United States<sup>§</sup>State Key Laboratory of Engines (SKLE) and <sup>||</sup>Collaborative Innovation Center of Chemical Science and Engineering, Tianjin University, Tianjin 300072, China<sup>⊥</sup>National Research Council Canada, Ottawa, Ontario K1A 0R6, Canada<sup>#</sup>ABQMR, 2301 Yale Boulevard SE, Albuquerque, New Mexico 87106, United States

**ABSTRACT:** Polymers of intrinsic microporosity (PIMs) can be functionalized with nitrogen-bearing groups, such as a nitrile group for PIM-1 and a methylated tetrazole group for MTZ-PIM, to physisorb CO<sub>2</sub>. Static <sup>13</sup>C NMR spectroscopy was used to investigate CO<sub>2</sub> dynamics by analysis of one-dimensional spectra and T<sub>2</sub> relaxation times at temperatures ranging from 6 to 295 K. Each polymer had two different loadings of CO<sub>2</sub> to determine the dominating relaxation mechanism at lower temperatures and deduce the identity of the weaker secondary adsorption site on the rigid polymer backbone. Both polymers, with a high loading of CO<sub>2</sub>, experience a narrowing of the <sup>13</sup>C NMR line width as the samples are warmed to 80 K, which is the onset of the weakly adsorbed CO<sub>2</sub> hopping on and off the polymer backbone.



## INTRODUCTION

The process of CO<sub>2</sub> capture is a set of strategies for reducing the emissions of carbon dioxide, with the goal of mitigating increased concentrations of atmospheric CO<sub>2</sub>.<sup>1–5</sup> Studies have focused on capturing CO<sub>2</sub> from mobile sources, such as automobiles, and large emitters, including power plants and cement factories.<sup>6,7</sup> The materials utilized here have potential applications as membrane capture materials for high-concentration emission sources, such as flue gases from power plants that burn hydrocarbon fuels. For coal-fired plants, these gas mixtures are typically composed of ~70% N<sub>2</sub>, ~15% CO<sub>2</sub>, and ~10% H<sub>2</sub>O.<sup>6</sup>

Current technologies for removing CO<sub>2</sub> from flue gas primarily use liquid amines,<sup>6,8–10</sup> in which CO<sub>2</sub> is bubbled through the solution, where it dissolves and reacts to form a chemisorbed product with the amine-bearing molecules. The solution-state capture materials have drawbacks such as amine leaching, chemical degradation, and high energy requirements for desorption and regeneration.<sup>6</sup> Solid adsorbents that physisorb CO<sub>2</sub>, such as those studied here, have been proposed as future carbon capture technologies because they will be able to avoid some of the limitations of current technologies.

Solid adsorbent materials exploit physisorption interactions to capture CO<sub>2</sub>. Physisorption of nitrogen-bearing sorbents relies on van der Waals interactions between an electron-rich adsorbing group and the electron-deficient carbon on the gas molecule to adsorb CO<sub>2</sub> molecules onto a surface. These interactions restrict (and likely stop) the motion of the

adsorbed CO<sub>2</sub> molecules but do not disrupt its electronic structure. Physisorption interactions have been shown to occur with CO<sub>2</sub> by metal–organic frameworks (MOFs)<sup>11–14</sup> and polymers of intrinsic microporosity (PIMs).<sup>15–20</sup> The PIMs studied here are depicted in Figure 1, which differ in the substitutions of the aryl backbone at two sites. Methyl tetrazole (MTZ)-PIM is prepared by a simple two-step reaction from PIM-1.<sup>18</sup>

Materials that exhibit CO<sub>2</sub> physisorption can be utilized as membrane capture technologies,<sup>15,21–25</sup> where CO<sub>2</sub> is separated from flue gas by attracting CO<sub>2</sub> preferentially through the

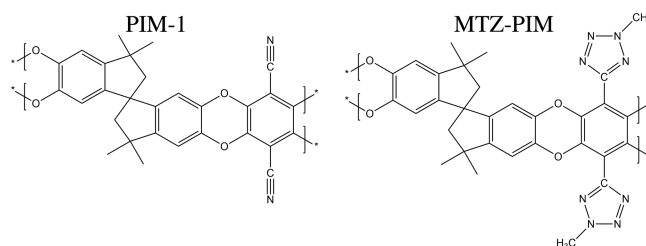


**Figure 1.** Structures of PIM-1 (left) and MTZ-PIM (right) polymers. PIM-1 has a nitrile-binding unit, whereas MTZ-PIM has a methyl tetrazole unit for adsorption of CO<sub>2</sub>.

Received: December 14, 2017

Revised: February 6, 2018

Published: February 7, 2018

material. Physisorption materials typically have a low energy requirement for regeneration of the adsorbing material due to the minimal energy required to overcome weak van der Waals interactions that attract the CO<sub>2</sub> molecules. As membrane capture materials, they can be used as efficient CO<sub>2</sub> capture technologies by balancing the selectivity and permeability of the material to allow preferential passage of CO<sub>2</sub>.

Solid-state NMR spectroscopy has been used to study a series of PIM adsorption materials. The polymers have micropores that allow for high gas permeability due to a combination of the rigid backbone and sites of contortion in the polymer chain that does not allow efficient chain packing. Once CO<sub>2</sub> gas has entered the pore space, it can be captured through interactions with the electron-rich adsorbing groups on the PIMs. Each sample has at least two adsorbing groups per repeating unit of polymer, which are randomly oriented within the polymer sample due to the contorted chain packing. PIM-1 has an electron-rich nitrile group that adsorbs CO<sub>2</sub> by interaction with the carbon in carbon dioxide, which is electron-deficient. Similar interactions have been modeled from ab initio studies and show an in-plane configuration of CO<sub>2</sub> with the nitrogen unit.<sup>26</sup> This interaction for both PIMs is depicted in Figure 2.

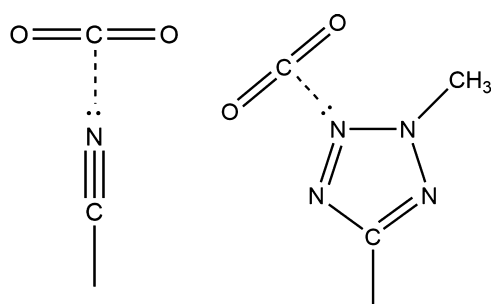


**Figure 2.** Depiction of nitrile unit from PIM-1 (left) and methyl tetrazole unit of MTZ-PIM (right) in van der Waals contact with CO<sub>2</sub>. The dashed line is a representation of the adsorption interaction.

The nitrile on PIM-1 can be replaced with more CO<sub>2</sub>-philic groups, such as tetrazole (TZ-PIM)<sup>15</sup> or methyl tetrazole (MTZ-PIM).<sup>18</sup> TZ-PIM was synthesized by a [2 + 3] cycloaddition postpolymerization reaction that has been previously described,<sup>15</sup> and MTZ-PIM was synthesized by methylating the tetrazole group of TZ-PIM.<sup>18</sup> MTZ-PIM, shown in Figure 2 (right), is able to adsorb CO<sub>2</sub> through the methyl tetrazole group at the 3-position, which is electron-rich.

In the present work, in situ <sup>13</sup>C NMR spectroscopy was used to study the adsorption of CO<sub>2</sub> on PIMs because it can detect and distinguish the gas-phase and adsorbed-phase <sup>13</sup>CO<sub>2</sub> within the material and report on dynamics using *T*<sub>2</sub> measurements. The study was done over a range of temperatures and with two loadings of <sup>13</sup>CO<sub>2</sub> for each of the PIM materials. The <sup>13</sup>C NMR line shapes and *T*<sub>2</sub> relaxation times were analyzed to give insights into the adsorption interactions present over the temperature and CO<sub>2</sub>-loading ranges. Combining information on the adsorption interactions from in situ <sup>13</sup>C NMR spectroscopy with macroscopic studies, including permeability, isotherms, and selectivity, will assist in improving current CO<sub>2</sub> separation technologies.

## MATERIALS AND METHODS

PIM samples underwent a bake-out procedure at 80 °C under vacuum for 24 h for degassing the polymer. Approximately 100–200 mg of the polymer sample was used for the NMR experiments. A known quantity, determined from isotherms,<sup>15,18</sup> of 99% <sup>13</sup>C-enriched CO<sub>2</sub> gas (Sigma-Aldrich) was introduced to the PIM samples for adsorption. To allow for thermal contact during the low-temperature experiments, 0.9 atm of helium gas was also introduced to the samples. After all of the gas was introduced to the sample, the tube for each sample was flame-sealed.

Variable-temperature <sup>13</sup>C NMR below 150 K was performed in a Kadel helium research dewar with a laboratory-built NMR probe. NMR studies above 150 K were performed with a second laboratory-built NMR probe, where cooling was provided by a temperature-regulated stream of evaporated liquid nitrogen. All data for the NMR studies were acquired using a Hahn echo<sup>27</sup> sequence with a  $\pi$  pulse length of 12  $\mu$ s. Depending on the temperature, a last delay of 5–35 s was used to acquire 64 transients for all spectra. The spectra were obtained via an echo pulse spacing ( $\tau$  delay) of 50  $\mu$ s. The lower signal-to-noise ratio in the low-loading samples arises from having fewer <sup>13</sup>C nuclei as fewer <sup>13</sup>CO<sub>2</sub> molecules were introduced to these samples.

## RESULTS AND DISCUSSION

The adsorption interactions were investigated by variable-temperature, static <sup>13</sup>C NMR spectroscopy with high and low CO<sub>2</sub>-loaded polymer samples. The “low-loading” samples of PIM-1 and MTZ-PIM were prepared with  $x = 0.33$  and  $0.34$ , respectively, where  $x$  represents the number of CO<sub>2</sub> molecules per binding unit of the PIMs, to generate a state where each CO<sub>2</sub> molecule has an available adsorbing site. The “high-loading” samples were loaded with  $x = 1.5$  for both samples, to provide an excess of CO<sub>2</sub> such that the gas molecules had to compete for the electron-rich adsorbing sites. An analysis of the pore size distribution of the related PIM-1 powder<sup>28</sup> shows the existence of microporous and mesoporous pores in a broad distribution of sizes ranging from approximately 0.6 to 12 nm. We anticipate only moderate differences between PIM-1 and MTZ-PIM; thus, we assume MTZ-PIM has a relatively similar pore size distribution as PIM-1. The packing of the polymer and the small pore sizes together result in a crowding effect that causes some adsorbing units to be sterically hindered and inaccessible for adsorption. However, the CO<sub>2</sub>-to-adsorbing unit ratio was calculated for the idealized condition that every adsorbing group in the sample is accessible. Therefore, there are additional CO<sub>2</sub> molecules present as compared to the available binding sites. Any CO<sub>2</sub> molecules that are not able to interact with an electron-rich adsorbing site will be forced to adsorb to less favorable adsorption sites within the polymer.

The temperature range studied was 6–295 K for each sample, where it can be assumed that a near-constant concentration of adsorbed CO<sub>2</sub> is covering the polymer (fixed quantity of <sup>13</sup>CO<sub>2</sub> in a sealed tube). This assumption can break down at higher temperatures, where some of the adsorbed CO<sub>2</sub> molecules could occupy the gas phase. However, the assumption of constant concentration can be made here because the void space volume within the sample tube, where gas-phase molecules can inhabit, is minimized. The setup here allows for an efficient study of adsorbed dynamics. In addition to constant CO<sub>2</sub> loading, the presence of the polymer

concentrates CO<sub>2</sub> in the sample space, meaning that the <sup>13</sup>C NMR signal intensity is much larger in the presence of the polymer than that in an identical tube filled only with <sup>13</sup>CO<sub>2</sub> gas.

Figure 3 depicts <sup>13</sup>C NMR spectra for the samples described above at representative temperatures from the study. Overall,

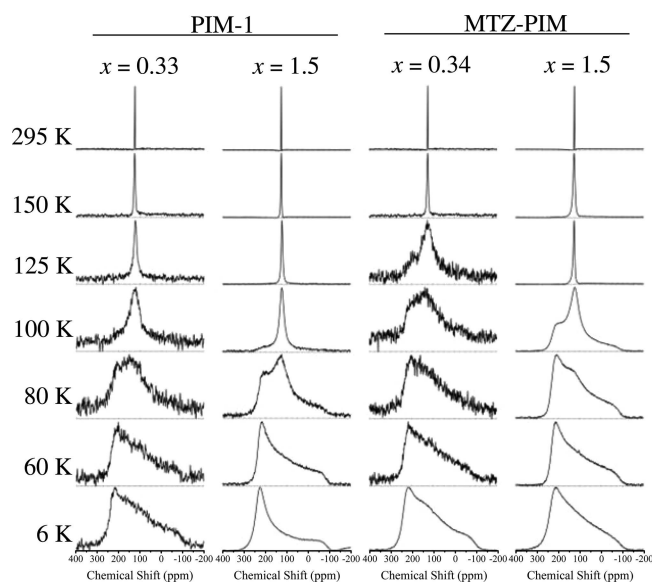


**Figure 3.** <sup>13</sup>C variable-temperature solid-state NMR spectra of CO<sub>2</sub> adsorbed on PIM-1 (left) and MTZ-PIM (right) samples, where *x* represents the number of CO<sub>2</sub> molecules per binding unit.

each sample is observed to have <sup>13</sup>C NMR line shape narrowing at increased temperatures. All measurements were conducted with a known amount of <sup>13</sup>CO<sub>2</sub>, equal number of scans, and under fully relaxed quantitative conditions ( $5 \times T_1$ , the spin–lattice relaxation time). Typical indications of physisorption in NMR spectra include an enhancement in signal (relative to gas alone filling the NMR sample space, indicating that the polymer concentrates the <sup>13</sup>CO<sub>2</sub> present) and a broadening of the resonance, both with no change in the isotropic chemical shift. These observable spectral features are due to the physisorption van der Waals interaction, which slows the motion of the CO<sub>2</sub> gas molecules without perturbing the CO<sub>2</sub> molecules' electronic environment. Compared to the line width of CO<sub>2</sub> gas, there is possibly some portion of the line broadening due to a minor effect from the magnetic susceptibility differences introduced by the PIM materials, particularly at high temperature, where the line is the narrowest.

The analysis of the <sup>13</sup>C NMR line shape data must begin by considering the nuclear spin interactions that can broaden the resonance of adsorbed <sup>13</sup>CO<sub>2</sub>. The line broadening of adsorbed <sup>13</sup>CO<sub>2</sub> is dominated by three such interactions. One is the chemical shift anisotropy (CSA),<sup>29</sup> which is characteristic of linear CO<sub>2</sub> molecules. The other two interactions are dipolar coupling interactions: <sup>1</sup>H–<sup>13</sup>C dipolar coupling between <sup>13</sup>CO<sub>2</sub> and the hydrogen atoms on the adsorbent polymer and <sup>13</sup>C–<sup>13</sup>C homonuclear dipolar coupling between two adsorbed <sup>13</sup>CO<sub>2</sub> molecules.

The dominant line-broadening mechanism at low temperatures, where CO<sub>2</sub> is static (not rotating on the NMR time scale of 10<sup>−4</sup> s), is the CSA. At 6 K, as described below, an additional source of line broadening is present. At low temperatures, all four samples have an axially symmetric

powder pattern in the <sup>13</sup>C NMR spectrum. This line shape is indicative of adsorbed CO<sub>2</sub> molecules on the PIM materials, and it arises because the <sup>13</sup>C tensor for the CO<sub>2</sub> molecule has only two unique principal values ( $\delta_{xx} = \delta_{yy}$  and  $\delta_{zz}$ ): two perpendicular to the C–O–C bond and one parallel to this bond. Previously, randomly oriented solid <sup>13</sup>CO<sub>2</sub> has been seen to exhibit a characteristic line shape,<sup>30,31</sup> which is similar to the resonance of the adsorbed <sup>13</sup>CO<sub>2</sub>. Therefore, it can be recognized that the orientation of adsorbed CO<sub>2</sub> molecules on the NMR time scale (10<sup>−4</sup> s) is nearly fixed with respect to the magnetic field. The <sup>13</sup>CO<sub>2</sub> molecules can have a random orientation because the PIM chain orientation is random in nature and the functional groups on the PIM samples have a fixed orientation with respect to the backbone. This means that the orientation of the functional groups is randomly distributed with respect to the magnetic field. Therefore, when CO<sub>2</sub> molecules are adsorbed on the polymer, they have a fixed molecular orientation with an isotropic distribution with respect to the magnetic field, which results in an axially symmetric CSA powder pattern.

To best describe the spectra below 80 K, the width of the CSA powder pattern,  $\Delta\sigma_{\text{eff}}$  should be measured. For both the PIM-1 and MTZ-PIM samples at 60 K, the  $\Delta\sigma_{\text{eff}}$  values are similar, 324.2 and 325.2 ppm, respectively. This is similar to the previously reported values for physisorbed CO<sub>2</sub> on TZ-PIM (290 ppm)<sup>32</sup> and an MOF (315.3 ppm)<sup>12–14</sup> as well as solid CO<sub>2</sub> (325 ppm).<sup>30</sup> A slight narrowing of the line shape in this temperature range is due to librational motions (orientational “wiggling”) within the adsorption site.<sup>32,33</sup> The librational motion is defined by the angle  $\theta$ , which is defined as that between the long axis of the CO<sub>2</sub> molecule and the axis of the energetically-preferred direction when adsorbed at the given site. Increasing the temperature creates a distribution of  $\theta$  values due to motion of the adsorbed CO<sub>2</sub> molecules within the adsorption site. This motion leads to a time-averaged CSA and a narrowing of the <sup>13</sup>C NMR spectra. The width of the CSA,  $\Delta\sigma_{\text{eff}}$  can be calculated by eq 1 because the line broadening is dominated by the CSA interaction.<sup>34</sup>

$$\Delta\sigma_{\text{eff}} = \Delta\sigma \left( \frac{3}{2} \overline{\cos^2 \theta} - \frac{1}{2} \right) \quad (1)$$

where  $\Delta\sigma$  is the full width of the CSA powder pattern when CO<sub>2</sub> is orientationally static. At the lowest temperatures,  $\theta = 0$  (neglecting quantum zero-point motion) and  $\Delta\sigma_{\text{eff}}$  is equal to  $\Delta\sigma$ . When  $\theta$  increases as the temperature increases, the  $\cos^2 \theta$  term decreases and the width of the CSA powder pattern slightly narrows. It is worth noting here that a “head-to-tail” flip of the adsorbed CO<sub>2</sub> molecule adds  $\pi$  to the angle  $\theta$ , leaving the cosine-squared term unchanged. Therefore, this flipping motion has no effect on the width of the CSA.

As the temperature is increased further, the adsorbed CO<sub>2</sub> molecules begin to reorient through translational hopping from one adsorption site to another. Figure 4 depicts the translation–reorientation hopping motion. Because every adsorption site has a unique alignment with respect to the magnetic field, the CO<sub>2</sub> molecules change orientation when the hop occurs. Therefore, the CSA powder pattern is averaged due to the motion. This narrowing due to the hopping motion is evident starting at 80–100 K in the samples. The line narrowing that occurs due to joint translation–reorientation hopping has been studied previously in solid CO<sub>2</sub>,<sup>30</sup>  $\alpha$ -CO,<sup>35</sup>

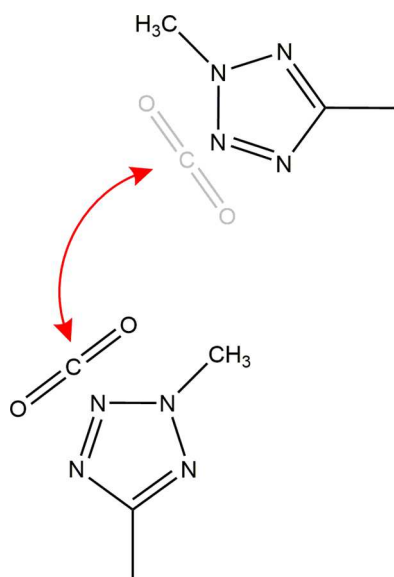


**Figure 4.** Translational–reorientation hopping of CO<sub>2</sub> from one methyl tetrazole binding unit to another on MTZ-PIM. A similar depiction can be shown for PIM-1, where CO<sub>2</sub> undergoes translational–reorientation hopping from one nitrile binding unit to another.

N<sub>2</sub>O,<sup>36</sup> and benzene<sup>37</sup> as well as CO<sub>2</sub> adsorbed on an MOF material<sup>12–14</sup> and TZ-PIM.<sup>32</sup>

As the temperature is increased further, the hopping motion becomes rapid on the NMR time scale, which time-averages the CSA interaction essentially to zero. With rapid CO<sub>2</sub> hopping between the orientationally random adsorption sites, the <sup>13</sup>C NMR spectrum is a single, symmetric resonance. This symmetric resonance continues to narrow as the temperature is increased further, indicating that the hopping motion continues to become more rapid. As the temperature increases, the van der Waals interactions that adsorb the CO<sub>2</sub> molecule to the electron-rich adsorbing group become smaller relative to the thermal energy of the system.

When adsorbed CO<sub>2</sub> molecules are tightly bound, at low temperatures, the line width is nearly constant for the CSA powder pattern. After the CO<sub>2</sub> molecules begin the site-to-site hopping mechanism, around 100 K, the line width decreases rapidly. The line width in both of the high-loading samples begins to narrow at a lower temperature (compared to the low-loading samples) and is slightly narrower during the onset of hopping because there are more weakly sorbed CO<sub>2</sub> molecules in these samples (the strongest binding sites are fully occupied, forcing some CO<sub>2</sub> to adsorb on weaker sites). Above 100 K, the high-temperature regime, the line width decreases due to rapid CO<sub>2</sub> reorientations that accompany the translational hopping mechanism. It is therefore unsurprising that the narrowing occurs at the lower temperature for both high-loading samples relative to the low-loading samples. MTZ-PIM retains more of a CSA-broadened component at 100–125 K, suggestive of stronger adsorption interactions relative to PIM-1 at those temperatures.

The <sup>13</sup>C NMR line shape analysis of CO<sub>2</sub> adsorbed on MTZ-PIM is similar to that seen previously on TZ-PIM.<sup>32</sup> CO<sub>2</sub> adsorbed on PIM-1 has similar trends but clearly does not adsorb CO<sub>2</sub> as strongly as MTZ-PIM. This is evidenced by the narrowing of the <sup>13</sup>C resonance in the low-loading samples by 100 K in the PIM-1 sample as opposed to 125 K in the MTZ-PIM sample. The variable-temperature study indicates differ-

ences in the hopping between the low- and high-loading samples for both polymers. The onset of site-to-site hopping for the low-loading samples of both PIM materials studied here occurs in a single step. These data indicate that each of the CO<sub>2</sub> molecules are adsorbed on similar sites, which must be the more favorable adsorbing sites because the first molecules will go to the lowest-energy sites. Alternatively, the high-loading samples have two steps to fully narrow the resonance, with the first near 80 K and the second near 125 K. This finding indicates that the high-loading samples have two subsets of CO<sub>2</sub> molecules, one that is more tightly adsorbed than the other. The more tightly adsorbed CO<sub>2</sub> molecules continue to be detected as a CSA powder pattern resonance. Because the two subsets have different affinities for CO<sub>2</sub>, it is presumed that they access two different adsorption sites.

At the lowest temperature, 6 K, the <sup>13</sup>C resonance broadens by a mechanism other than the CSA interaction and has an increase in signal-to-noise ratio (due to the 1/*T* nuclear magnetization). The general shape of the CSA powder pattern can still be seen, but there is an overall broadening of the features; this is most obvious in the high-loading MTZ-PIM sample (compare 6 and 60 K spectra). At these temperatures, the broadening mechanism is not able to be ascribed to molecular motions because they are frozen out at 80 K. Therefore, we attribute this broadening to the magnetic susceptibility of electrons in the material, as described for CO<sub>2</sub> adsorption on TZ-PIM<sup>32</sup> and seen in Mg-MOF-74.<sup>12–14</sup> Probably, this is from paramagnetic impurity centers.

The <sup>13</sup>C spin–spin (transverse) relaxation time, *T*<sub>2</sub>, was measured across the same temperature range to assist in determining the mechanisms of line narrowing at each temperature.<sup>30,38</sup> These data are shown in Figure 5, and both plots look very similar.<sup>30,38</sup>

The dipolar coupling interactions (<sup>1</sup>H–<sup>13</sup>C and <sup>13</sup>C–<sup>13</sup>C) and molecular motions both contribute to the measured *T*<sub>2</sub> for adsorbed CO<sub>2</sub>. When dipolar coupling is present, it is observed by NMR spectroscopy through echo attenuation, which leads to a shorter *T*<sub>2</sub>. Alternatively, if the dipolar coupling is averaged to zero, the signal is not attenuated and the *T*<sub>2</sub> remains long. In the low-temperature range, the relaxation is determined by the <sup>13</sup>C–<sup>13</sup>C dipolar coupling between adsorbed <sup>13</sup>CO<sub>2</sub> molecules and the <sup>13</sup>C–<sup>1</sup>H dipolar coupling between an adsorbed CO<sub>2</sub> molecule and hydrogen from the adsorbing group. There is no apparent change in *T*<sub>2</sub> with different loadings of CO<sub>2</sub>, indicating that the <sup>1</sup>H–<sup>13</sup>C dipolar interaction dominates the relaxation mechanism. In this temperature range, there are no CO<sub>2</sub> translations to average out these dipolar interactions, as has been previously described.<sup>32</sup> From 6 to 60 K, the *T*<sub>2</sub> values in all samples are consistent, indicating that the dipolar coupling is not changing with temperature because the CO<sub>2</sub> hopping motion is frozen out in this temperature range.

Around 60 K, the *T*<sub>2</sub> relaxation begins to decrease due to the onset of CO<sub>2</sub> reorientational motion.<sup>30,35</sup> This temperature regime from 60 to 125 K, the strong collision regime,<sup>35,39</sup> is defined by a CO<sub>2</sub> molecule undergoing a single reorientation, which causes the <sup>13</sup>C spin to lose coherence, changing the frequency and therefore attenuating the echo signal, resulting in a decreased *T*<sub>2</sub>. The mean time between hopping events is approximately the *T*<sub>2</sub> relaxation time in this intermediate temperature range. *T*<sub>2</sub> stops decreasing when molecular hops occur approximately once during the rigid-lattice free induction decay, which is approximately 100 μs.<sup>50</sup> For higher hop rates, line narrowing occurs and *T*<sub>2</sub> increases. The high-loading PIM

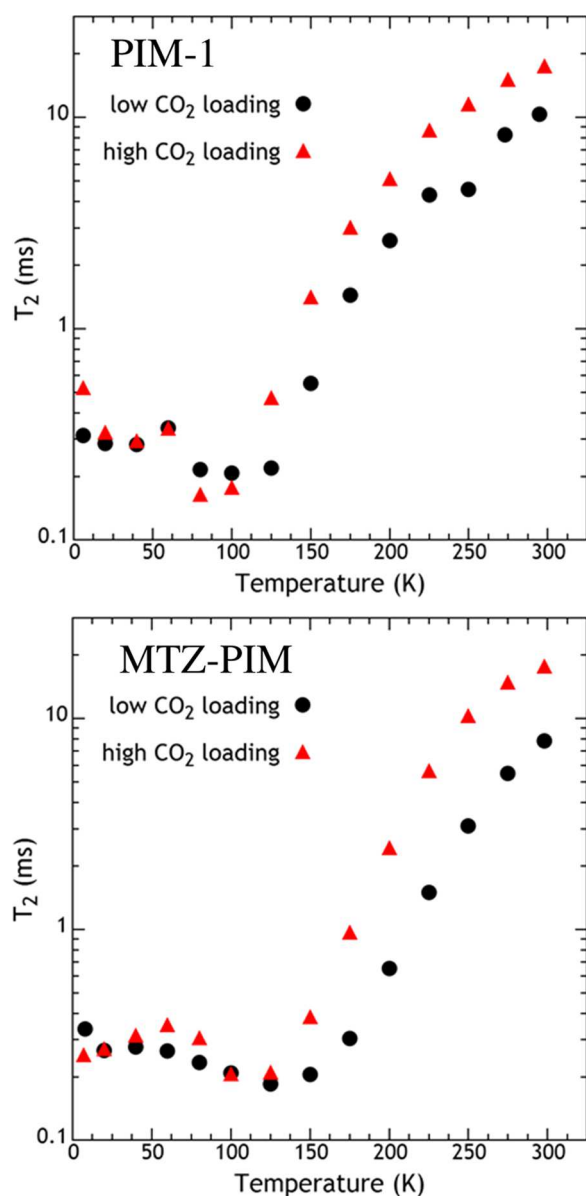


**Figure 5.** Semilogarithmic plot of  $T_2$  relaxation times (ms) vs. temperature for the PIM-1 (top) and MTZ-PIM (bottom) samples.

samples show an earlier onset of increase of  $T_2$  relaxation time (i.e., at a lower temperature) compared to the low-loading PIM samples. This lower-temperature threshold is due to the subset of  $\text{CO}_2$  molecules that are adsorbed on the weaker adsorption sites and therefore begin hopping at a lower temperature. The  $T_2$  values for the PIM-1 samples begin to increase around 100 K, whereas those for the MTZ-PIM samples begin to increase around 125 K. This difference is caused by the greater strength of adsorption for the methyl tetrazole-adsorbing groups.

In the high-temperature regime (above 125 K), the  $\text{CO}_2$  molecules undergo fast reorientational hopping as well as translational hops. This motion causes the  $T_2$  to increase as the temperature rises. The mechanism of site-to-site hopping is confirmed when the  $T_2$  value surpasses the low-temperature  $T_2$  plateau, near 150 K. The plateau was determined by dipolar coupling, which required the  $\text{CO}_2$  molecule to be located at a single adsorption site. These dipolar couplings are averaged to zero by the fast translational hopping at these temperatures.

In both PIM samples, the onset of hopping from the weakly adsorbed  $\text{CO}_2$  molecules is evident at 80 K and the hopping occurs rapidly at 100 K. This result is demonstrated by the CSA powder pattern being averaged to zero. Because weakly adsorbed  $\text{CO}_2$  molecules on both PIM-1 and MTZ-PIM exhibit a comparable hopping mechanism, also shown for TZ-PIM previously,<sup>32</sup> the second adsorption site on each polymer must be similar. When comparing the structure of these polymer samples, as shown in Figure 1, the consistent moiety in each sample is the polymer backbone. Hence, we conclude that the functional group is not responsible for the binding of the secondary adsorption site and that the weakly adsorbed  $\text{CO}_2$  molecules are binding to the polymer chain. If this site would have also been on the adsorbing unit, it would be expected to be absent on at least the PIM-1 samples, as the nitrile group would not support two adsorbed  $\text{CO}_2$  molecules.

## CONCLUSIONS

In this variable-temperature NMR study, it has been shown that  $\text{CO}_2$  undergoes translation–reorientation hopping between the adsorption sites of PIM-1 and MTZ-PIM. The data show that the site-to-site hopping starts with infrequent jumps at 80 K for the PIM-1 sample and at 100 K for the MTZ-PIM sample. This finding indicates that  $\text{CO}_2$  is more tightly adsorbed in the methyl tetrazole-containing sample as opposed to PIM-1. The  $^{13}\text{C}$  NMR CSA powder pattern is time-averaged above 150 K, which indicates that above this temperature the hopping mechanism has become rapid (faster than  $10^5 \text{ s}^{-1}$ ) for all samples. It can also be seen in the lower-temperature range that a second adsorption site is found in both samples when there is an excess of  $\text{CO}_2$  introduced to the polymer sample. This second adsorption site does not bind  $\text{CO}_2$  as tightly, evidenced by the  $^{13}\text{C}$  resonance narrowing at a lower temperature due to hopping. From these data, it is apparent that the second adsorption site is conserved between both PIM-1 and MTZ-PIM materials. The conserved moiety in these samples, as well as the previously studied TZ-PIM,<sup>32</sup> is the PIM backbone. Therefore, the data suggest that the weakly adsorbing site is an electron-rich region of the polymer itself (likely the benzodioxane ring), as opposed to being on the functional groups that distinguish these three materials (polymers) from one another.

## AUTHOR INFORMATION

### Corresponding Author

\*E-mail: [hayes@wustl.edu](mailto:hayes@wustl.edu). Phone: 314-935-4624.

### ORCID

Robert M. Marti: 0000-0003-0334-4135

Michael D. Guiver: 0000-0003-2619-6809

Sophia E. Hayes: 0000-0002-2809-6193

### Notes

The authors declare no competing financial interest.

## ACKNOWLEDGMENTS

This work was supported, in part, by the Center for Understanding and Control of Acid Gas-Induced Evolution of Materials for Energy (UNCAGE-ME), an Energy Frontier Research Center funded by the U.S. Department of Energy, Office of Science, Basic Energy Sciences under Award No. DE-SC0012577.

## REFERENCES

- (1) Didas, S. A.; Kulkarni, A. R.; Sholl, D. S.; Jones, C. W. Role of Amine Structure on Carbon Dioxide Adsorption from Ultradilute Gas Streams such as Ambient Air. *ChemSusChem* **2012**, *5*, 2058–2064.
- (2) Hicks, J. C.; Drese, J. H.; Fauth, D. J.; Gray, M. L.; Qi, G.; Jones, C. W. Designing Adsorbents for CO<sub>2</sub> Capture from Flue Gas-Hyperbranched Aminosilicas Capable of Capturing CO<sub>2</sub> Reversibly. *J. Am. Chem. Soc.* **2008**, *130*, 2902–2903.
- (3) Samanta, A.; Zhao, A.; Shimizu, G. K. H.; Sarkar, P.; Gupta, R. Post-Combustion CO<sub>2</sub> Capture Using Solid Sorbents: A Review. *Ind. Eng. Chem. Res.* **2012**, *51*, 1438–1463.
- (4) Choi, S.; Drese, J. H.; Jones, C. W. Adsorbent Materials for Carbon Dioxide Capture from Large Anthropogenic Point Sources. *ChemSusChem* **2009**, *2*, 796–854.
- (5) Schuiling, R. D.; de Boer, P. L. Six Commercially Viable Ways to Remove CO<sub>2</sub> from the Atmosphere And/or Reduce CO<sub>2</sub> Emissions. *Environ. Sci. Eur.* **2013**, *25*, No. 35.
- (6) Bhowan, A. S.; Freeman, B. C. Analysis and Status of Post-Combustion Carbon Dioxide Capture Technologies. *Environ. Sci. Technol.* **2011**, *45*, 8624–8632.
- (7) Jones, C. W. CO<sub>2</sub> Capture from Dilute Gases as a Component of Modern Global Carbon Management. *Annu. Rev. Chem. Biomol. Eng.* **2011**, *2*, 31–52.
- (8) Sharma, S.; Azzi, M. A Critical Review of Existing Strategies for Emission Control in the Monoethanolamine-Based Carbon Capture Process and Some Recommendations for Improved Strategies. *Fuel* **2014**, *121*, 178–188.
- (9) Yang, Q.; Bown, M.; Ali, A.; Winkler, D.; Puxty, G.; Attalla, M. A Carbon-13 NMR Study of Carbon Dioxide Absorption and Desorption with Aqueous Amine Solutions. *Energy Procedia* **2009**, *1*, 955–962.
- (10) Mani, F.; Peruzzini, M.; Stoppioni, P. CO<sub>2</sub> Absorption by Aqueous NH<sub>3</sub> Solutions: Speciation of Ammonium Carbamate, Bicarbonate and Carbonate by a <sup>13</sup>C NMR Study. *Green Chem.* **2006**, *8*, 995–1000.
- (11) Queen, W. L.; Brown, C. M.; Britt, D. K.; Zajdel, P.; Hudson, M. R.; Yaghi, O. M. Site-Specific CO<sub>2</sub> Adsorption and Zero Thermal Expansion in an Anisotropic Pore Network. *J. Phys. Chem. C* **2011**, *115*, 24915–24919.
- (12) Kong, X.; Scott, E.; Ding, W.; Mason, J. A.; Long, J. R.; Reimer, J. A. CO<sub>2</sub> Dynamics in a Metal-Organic Framework with Open Metal Sites. *J. Am. Chem. Soc.* **2012**, *134*, 14341–14344.
- (13) Lin, L.-C.; Kim, J.; Kong, X.; Scott, E.; McDonald, T. M.; Long, J. R.; Reimer, J. A.; Smit, B. Understanding CO<sub>2</sub> Dynamics in Metal-Organic Frameworks with Open Metal Sites. *Angew. Chem., Int. Ed.* **2013**, *52*, 4410–4413.
- (14) Marti, R. M.; Howe, J. D.; Morelock, C. R.; Conradi, M. S.; Walton, K. S.; Sholl, D. S.; Hayes, S. E. CO<sub>2</sub> Dynamics in Pure and Mixed-Metal MOFs with Open Metal Sites. *J. Phys. Chem. C* **2017**, *121*, 25778–25787.
- (15) Du, N.; Park, H. B.; Robertson, G. P.; Dal-Cin, M. M.; Visser, T.; Scoles, L.; Guiver, M. D. Polymer Nanosieve Membranes for CO<sub>2</sub>-Capture Applications. *Nat. Mater.* **2011**, *10*, 372–375.
- (16) Budd, P. M.; Elabas, E. S.; Ghanem, B. S.; Makhseed, S.; McKeown, N. B.; Msayib, K. J.; Tattershall, C. E.; Wang, D. Solution-Processed, Organophilic Membrane Derived from a Polymer of Intrinsic Microporosity. *Adv. Mater.* **2004**, *16*, 456–459.
- (17) Budd, P. M.; Ghanem, B. S.; Makhseed, S.; McKeown, N. B.; Msayib, K. J.; Tattershall, C. E. Polymers of Intrinsic Microporosity (PIMs): Robust, Solution-Processable, Organic Nanoporous Materials. *Chem. Commun.* **2004**, 230–231.
- (18) Du, N.; Robertson, G. P.; Dal-Cin, M. M.; Scoles, L.; Guiver, M. D. Polymers of Intrinsic Microporosity (PIMs) Substituted with Methyl Tetrazole. *Polymer* **2012**, *53*, 4367–4372.
- (19) Gameda, A. E.; De Angelis, M. G.; Du, N.; Li, N.; Guiver, M. D.; Sarti, G. C. Mixed Gas Sorption in Glassy Polymeric Membranes. III. CO<sub>2</sub>/CH<sub>4</sub> Mixtures in a Polymer of Intrinsic Microporosity (PIM-1): Effect of Temperature. *J. Membr. Sci.* **2017**, *524*, 746–757.
- (20) Wang, S.; Li, X.; Wu, H.; Tian, Z.; Xin, Q.; He, G.; Peng, D.; Chen, S.; Yin, Y.; Jiang, Z.; et al. Advances in High Permeability Polymer-Based Membrane Materials for CO<sub>2</sub> Separations. *Energy Environ. Sci.* **2016**, *9*, 1863–1890.
- (21) Guiver, M. D.; Lee, Y. M. Polymer Rigidity Improves Microporous Membranes. *Science* **2013**, *339*, 284–285.
- (22) Du, N.; Park, B.; Dal-Cin, M. M.; Guiver, M. D. Advances in High Permeability Polymeric Membrane Materials for CO<sub>2</sub>. *Energy Environ. Sci.* **2012**, *5*, 7306–7322.
- (23) Lin, H.; Freeman, B. D. Materials Selection Guidelines for Membranes That Remove CO<sub>2</sub> from Gas Mixtures. *J. Mol. Struct.* **2005**, *739*, 57–74.
- (24) Merkel, T. C.; Lin, H.; Wei, X.; Baker, R. Power Plant Post-Combustion Carbon Dioxide Capture: An Opportunity for Membranes. *J. Membr. Sci.* **2010**, *359*, 126–139.
- (25) Shao, P.; Dal-Cin, M. M.; Guiver, M. D.; Kumar, A. Simulation of Membrane-Based CO<sub>2</sub> Capture in a Coal-Fired Power Plant. *J. Membr. Sci.* **2013**, *427*, 451–459.
- (26) Vogiatzis, K. D.; Mavrandonakis, A.; Klopper, W.; Froudakis, G. E. Ab Initio Study of the Interactions between CO<sub>2</sub> and N-Containing Organic Heterocycles. *ChemPhysChem* **2009**, *10*, 374–383.
- (27) Hahn, E. L. Spin Echoes. *Phys. Rev.* **1950**, *80*, 580–594.
- (28) Polak-Kraśna, K.; Dawson, R.; Holyfield, L. T.; Bowen, C. R.; Burrows, A. D.; Mays, T. J. Mechanical Characterisation of Polymer of Intrinsic Microporosity PIM-1 for Hydrogen Storage Applications. *J. Mater. Sci.* **2017**, *52*, 3862–3875.
- (29) Fukushima, E.; Roeder, S. B. W. *Experimental Pulse NMR: A Nuts and Bolts Approach*; Addison-Wesley Publishing Company, 1981.
- (30) Liu, S. B.; Doverspike, M. A.; Conradi, M. S. Combined Translation-Rotation Jumps in Solid Carbon Dioxide. *J. Chem. Phys.* **1984**, *81*, 6064–6068.
- (31) Ratcliffe, C. I.; Ripmeester, J. A. <sup>1</sup>H and <sup>13</sup>C NMR Studies on Carbon Dioxide Hydrate. *J. Phys. Chem.* **1986**, *90*, 1259–1263.
- (32) Moore, J. K.; Guiver, M. D.; Du, N.; Hayes, S. E.; Conradi, M. S. Molecular Motions of Adsorbed CO<sub>2</sub> on a Tetrazole-Functionalized PIM Polymer Studied with <sup>13</sup>C NMR. *J. Phys. Chem. C* **2013**, *117*, 22995–22999.
- (33) Bayer, H. Theory of Spin-Lattice Relaxation in Molecular Crystals. *Z. Physik* **1951**, *130*, 227–238.
- (34) Mehring, M. *Principles of High Resolution NMR in Solids*, 2nd ed.; Springer, 1983.
- (35) Liu, S.; Conradi, M. S. Combined Translational-Rotational Jumps in Solid Alpha-CO. *Phys. Rev. B* **1984**, *30*, 24–31.
- (36) Ouyang, B.; Conradi, M. S. Nuclear-Magnetic-Resonance Determination of the Mechanism of Molecular Reorientation in Solid N<sub>2</sub>O. *Phys. Rev. B* **1991**, *44*, No. 9295.
- (37) Gullion, T.; Conradi, M. S. Anisotropic Diffusion in Benzene: <sup>13</sup>C NMR Study. *Phys. Rev. B* **1985**, *32*, No. 7076.
- (38) Rothwell, W. P.; Waugh, J. S. Transverse Relaxation of Dipolar Coupled Spin Systems under Rf Irradiation: Detecting Motions in Solids. *J. Chem. Phys.* **1981**, *74*, 2721–2732.
- (39) Slichter, C. P. *Principles of Magnetic Resonance*, 3rd ed.; Springer, 1990.